Available online at www.sciencedirect.com
ScienceDirect
Journal of Sound and Vibration 308 (2007) 758–766
JOURNAL OF SOUND AND VIBRATION
www.elsevier.com/locate/jsvi

Stiffening effect of the rotor during the rotor-to-stator rub in a rotating machine

Fulei Chu*, Wenxiu Lu

Department of Precision Instruments, Tsinghua University, Beijing 100084, China

Accepted 22 March 2007
The peer review of this article was organized by the Guest Editor
Available online 1 June 2007

Abstract

Rotor-to-stator rub is one of the common malfunctions in rotating machinery. When rub–impact occurs, the transient dynamic change of the natural frequencies of the system will appear. This change actually reflects the stiffening effect of the rotor during the rotor-to-stator rub. In this paper, the dynamic model of the rubbing rotor system is established and the dynamics of the rubbing rotor is investigated. The parameter identification is used to process the vibration data obtained by numerical simulation and experimental test. The change in the transient stiffness of the rotor is analyzed and the stiffening effect of the rotor is investigated quantitatively. It is found that the change of the transient stiffness can effectively reflect the severity of the rub–impact.

1. Introduction

In gas turbine generating sets and other high-speed rotating machines the clearance between rotor and stator becomes smaller and smaller with the need of high speed and high efficiency. This has led to the frequent occurrence of the rotor-to-stator rub, especially between the rotor and seal or the blade tip and the envelope. Rotor-to-stator rub is usually a secondary phenomenon resulting from other faults. It will cause very complicated vibration to the rotor system and is one of the main reasons for the system instability. When it occurs severe vibration will be induced in the equipments at least. And at worst it will lead to the permanent bow to the shaft, and even the damage to the whole shaft system.

Effective and accurate diagnostics to the rub–impact can avoid serious accidents caused by this fault. On the other hand, early detection of the fault can shorten the maintenance time and this will produce great economic benefit. For the diagnostics of the rub–impact in rotating machines, the complicated dynamic phenomenon and various extracted features are the basis for the accurate diagnostics. For the research on motion stability and dynamics characteristics of the rub–impact rotor system, Ehrich [1] studied the cases of the rub–impact between the shaft and the bearing and the rub–impact between the rotor and the stator near supports at two ends of the Jeffcott rotor system. Zhang et al. [2] analyzed the rub–impact caused by geometric asymmetry between the rotor and stator, and studied the grazing phenomenon of the single point rubbing in detail. Liu [3] analyzed

*Corresponding author.
E-mail address: chufl@mail.tsinghua.edu.cn (F. Chu).

0022-460X/$ - see front matter © 2007 Elsevier Ltd. All rights reserved.
doi:10.1016/j.jsv.2007.03.059

several typical models of the rub–impact, and studied chaotic characteristics of the local rubbing. Dai et al. [4] designed an experiment of rotor/stop rubbing, and analyzed its vibration responses. Li et al. [5] analyzed the nonlinear dynamics behavior of the rub–impact between the single rotor supported by oil film bearings and the elastic stator. Much research has been performed on the fault features of the rub–impact rotor system.

In the experiment of the rub–impact rotor system, it is often discovered that the transient natural frequencies change once the rubbing occurs. This change is caused actually by the increase of the transient stiffness of the rotor. But up to now, based on authors' knowledge, there is no investigation on the quantitative description of the transient stiffness and the characteristics it may manifest.

This paper will focus on the rub–impact malfunction of the rotor system. When rub–impact occurs in the system, it will produce a stiffening effect on rotor, and increase the transient stiffness. Therefore, the value of this transient stiffness can be identified by simulation or experimental vibration data with parameter identification theory. In the identification process, the rub–impact effect can be ignored and be reflected with the value of this transient stiffness even if the rub–impact occurs. The value of the transient stiffness is calculated when rub–impact occurs, and a quantitative analysis of the stiffening effect of the rotor is then given by numerical simulation and experiment data.

2. Theoretical basis

When a rotor system has rub–impact, it will be acted by both the friction force and the impact force. This will cause complicated motions in the system. Since the interaction between the rotor and stator equals to the addition of a transient support to the rotor, the transient stiffness of the system increases. Once the contact stops, the transient stiffness of the system returns to the normal steady value just like the case when there is no rub–impact. To describe the stiffening effect of the rotor when the rub–impact occurs, an equivalent stiffness (called transient stiffness) is used to reflect the total effect of this time-varying stiffness on the system. In this way, the stiffening effect of the rotor can be analyzed quantitatively.

The basic idea using the definition of the transient stiffness is: firstly establish the differential equations of motion for the rotor system with rub–impact, then describe the effect of the rub–impact interaction on the rotor system by transient stiffness and damping, namely to take the rotor system as a mass-stiffness-damping system without rub–impact, and finally identify this transient stiffness with parameter identification. By investigating the change trend of the transient stiffness with the rotating speed, the stiffening effect of the rotor can be described quantitatively.

The above figure is of a rub–impact Jeffcott rotor system (Fig. 1). The differential equations of motion for the system can be established as

$$\begin{cases} m\ddot{x}(t) + c_0\dot{x}(t) + k_0x(t) = F_{ux}(t) + F_{fx}(t), \\ m\ddot{y}(t) + c_0\dot{y}(t) + k_0y(t) = F_{uy}(t) - F_g + F_{fy}(t), \end{cases} \tag{1}$$

where k_0 is the coefficient of the inherent stiffness of the shaft, c_0 the coefficient of the inherent damping of the system, m the mass, F_{ux} the imbalance force in x direction caused by the imbalance u, F_{uy} the imbalance force in y direction caused by the imbalance u, F_{fx} the rub–impact force in x direction, F_{fy} the rub–impact force in y direction, F_g the gravity, x, y the radial displacements of the disk, t the time and the dots express derivations to time.

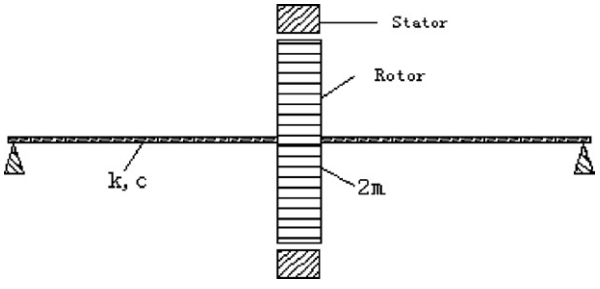

Fig. 1. Diagram of a rub–impact Jeffcott rotor system.

Now, the effect of rub–impact on the rotor system is reflected by the transient stiffness. Therefore, the rotor system can be considered as a mass-stiffness-damping system without the rub–impact interaction, and differential equations for the system can then be written as

$$\begin{cases} m\ddot{x}(t) + c\dot{x}(t) + kx(t) = F_{ux}(t), \\ m\ddot{y}(t) + c\dot{y}(t) + ky(t) = F_{uy}(t) - F_g, \end{cases} \tag{2}$$

where $F_{ux} = mu\omega^2 \cos(\omega t)$, $F_{uy} = mu\omega^2 \sin(\omega t)$, k the transient stiffness coefficient, and c the transient damping coefficient.

The identification equation in frequency domain can be obtained from Eq. (2) as

$$\begin{cases} -m\omega^2 x(\omega) + j\omega c x(\omega) + kx(\omega) = F_{ux}(\omega), \\ -m\omega^2 y(\omega) + j\omega c y(\omega) + ky(\omega) = F_{uy}(\omega) - F_g. \end{cases} \tag{3}$$

Its discrete form is

$$\begin{cases} jn\omega_0 cx(n\omega_0) + kx(n\omega_0) = F_{ux}(n\omega_0) + m(n\omega_0)^2 x(n\omega_0), \\ jn\omega_0 cy(n\omega_0) + ky(n\omega_0) = F_{uy}(n\omega_0) + m(n\omega_0)^2 y(n\omega_0), \end{cases} \tag{4}$$

where $n = 1, 2, \ldots, N/2$, ω_0 the resolution of frequency, and N the length of the time series $x(t)$. Suppose

$$B_1(n) = mn^2\omega_0^2 x(n\omega_0) + F_{ux}(n\omega_0),$$
$$B_2(n) = mn^2\omega_0^2 y(n\omega_0) + F_{uy}(n\omega_0)$$

and let the counterparts of real part and imaginary part in both sides of Eq. (4) equal, then

$$\begin{cases} -n\omega_0 c\,\mathrm{Im}(x(n\omega_0)) + k\,\mathrm{Re}(x(n\omega_0)) = \mathrm{Re}(B_1(n)), \\ n\omega_0 c\,\mathrm{Re}(x(n\omega_0)) + k\,\mathrm{Im}(x(n\omega_0)) = \mathrm{Im}(B_1(n)), \\ -n\omega_0 c\,\mathrm{Im}(y(n\omega_0)) + k\,\mathrm{Re}(y(n\omega_0)) = \mathrm{Re}(B_2(n)), \\ n\omega_0 c\,\mathrm{Re}(y(n\omega_0)) + k\,\mathrm{Im}(y(n\omega_0)) = \mathrm{Im}(B_2(n)). \end{cases} \tag{5}$$

Therefore, the identification equation can be obtained [6]:

$$\mathbf{As} = \mathbf{b}, \tag{6}$$

where $\mathbf{s} = (c, k)^{\mathrm{T}}$

$$\mathbf{A} = \begin{Bmatrix} -\omega_0\,\mathrm{Im}(x(\omega_0)) & \mathrm{Re}(x(\omega_0)) \\ \omega_0\,\mathrm{Re}(x(\omega_0)) & \mathrm{Im}(x(\omega_0)) \\ -\omega_0\,\mathrm{Im}(y(\omega_0)) & \mathrm{Re}(y(\omega_0)) \\ \omega_0\,\mathrm{Re}(y(\omega_0)) & \mathrm{Im}(y(\omega_0)) \\ \vdots & \vdots \\ -\frac{N}{2}\omega_0 \mathrm{Im}\left(x\left(\frac{N}{2}\omega_0\right)\right) & \mathrm{Re}\left(x\left(\frac{N}{2}\omega_0\right)\right) \\ \frac{N}{2}\omega_0 \mathrm{Re}\left(x\left(\frac{N}{2}\omega_0\right)\right) & \mathrm{Im}\left(x\left(\frac{N}{2}\omega_0\right)\right) \\ -\frac{N}{2}\omega_0 \mathrm{Im}\left(y\left(\frac{N}{2}\omega_0\right)\right) & \mathrm{Re}\left(y\left(\frac{N}{2}\omega_0\right)\right) \\ \frac{N}{2}\omega_0 \mathrm{Re}\left(y\left(\frac{N}{2}\omega_0\right)\right) & \mathrm{Im}\left(y\left(\frac{N}{2}\omega_0\right)\right) \end{Bmatrix},$$

$$\mathbf{b} = \begin{Bmatrix} \mathrm{Re}(B_1(1)) \\ \mathrm{Im}(B_1(1)) \\ \mathrm{Re}(B_2(1)) \\ \mathrm{Im}(B_2(1)) \\ \vdots \\ \mathrm{Re}\left(B_1\left(\frac{N}{2}\right)\right) \\ \mathrm{Im}\left(B_1\left(\frac{N}{2}\right)\right) \\ \mathrm{Re}\left(B_2\left(\frac{N}{2}\right)\right) \\ \mathrm{Im}\left(B_2\left(\frac{N}{2}\right)\right) \end{Bmatrix}.$$

With Eq. (6), undetermined coefficients **s** can be fitted by some methods such like the least square method, and therefore the transient stiffness coefficient k and the transient damping coefficient c can then be obtained.

3. Identification of transient stiffness based on simulation data

It is assumed that there is an initial clearance of δ between rotor and stator. Compared with one complete period of rotating, the time during rub–impact is very short, therefore, an elastic impact model is used. Also, the Coulomb type of frictional relationship is assumed in the simulation. In Eq. (1), the differential equations for the single Jeffcott rotor system are established. When rubbing happens, the rubbing force can be expressed as

$$\begin{Bmatrix} F_{fx} \\ F_{fy} \end{Bmatrix} = H\frac{(e-\delta)k_c}{e}\begin{bmatrix} 1 & -f \\ f & 1 \end{bmatrix}\begin{bmatrix} x \\ y \end{bmatrix},$$

where

$$H = \begin{cases} 0 & (e \leqslant \delta) \\ -1 & (e > \delta) \end{cases},$$

δ is the clearance between the rotor and stator, f the friction coefficient between the rotor and stator, k_c the radial stiffness of the stator, $e = \sqrt{x^2 + y^2}$ is the radial displacement of the rotor. The above equation indicates that when the rotor displacement e is smaller than δ, the static clearance between rotor and stator, there will be no rub–impact interaction and the rub–impact forces are zero while the rub–impacting will happen if the rotor displacement e is bigger than δ.

Based on Eq. (1), vibration response data of the system can be obtained by the fourth-order Runge–Kutta method. Then simulation data are identified by the above-mentioned model-based identification method, consequently the transient stiffness of the system can be obtained, and the stiffening effect of the rotor while rub–impact occurs can be observed.

Example 1: The rotor system is rigidly supported in both ends, some parameters used are: mass $m = 0.6116\,\mathrm{kg}$, damping coefficient $c_0 = 53\,\mathrm{N\,s/m}$, stiffness coefficient $k_0 = 7.3 \times 10^4\,\mathrm{N/m}$, stiffness coefficient of the stator $k_c = 5 \times 10^7\,\mathrm{N/m}$, clearance between the rotor and stator $\delta = 2.6 \times 10^{-4}\,\mathrm{m}$, friction coefficient $f = 0.18$, imbalance $u = 1 \times 10^{-4}\,\mathrm{m}$.

During the simulation process, it can be found that the rub–impact between the rotor and stator begins to occur at a time about when $n = 2860\,\mathrm{rev/min}$. By the obtained simulation data, the identification result of the transient stiffness coefficient is shown in Fig. 2, from which it can be seen that there is a slight increase of k

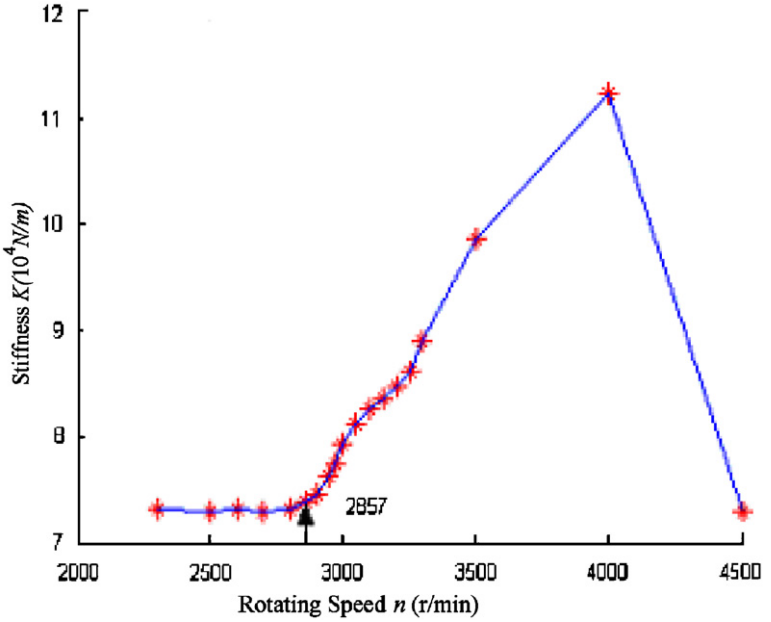

Fig. 2. Identification result of the transient stiffness.

when rub–impact occurs, i.e. $n = 2860$ rev/min. With the rub–impact aggravating, k keeps on increasing. When rub–impact stops, i.e. $n = 4500$ rev/min, k resumes to its original value. It is shown that with the rub–impact occurred, there appeared obvious stiffening effect of the rotor, which is then intensified with the rub–impact aggravating and disappeared after the rub–impact stopping.

Example 2: The rotor system is supported in both ends by oil film bearings. Some parameters used are mass $m = 0.6143$ kg, damping coefficient $c_0 = 53$ N s/m, stiffness coefficient $k_0 = 7.1 \times 10^4$ N/m, stiffness coefficient of the stator $k_c = 5 \times 10^7$ N/m, clearance between the rotor and stator $\delta = 2.6 \times 10^{-4}$ m, friction coefficient $f = 0.18$, imbalance $u = 1 \times 10^{-4}$ m, oil film viscosity $\eta = 0.06$ Pa., bearing clearance $c_1 = 3 \times 10^{-4}$ m, rotor radius $R = 0.033$ m, and bearing length $l = 0.365$ m.

When the rotor is supported by oil film bearings, the differential equations of the system are [7]

$$\begin{cases} m\ddot{x}_1 + c(\dot{x}_1 - \dot{x}_2) + k(x_1 - x_2) = F_{fx}(x_1, x_2) + mu\omega^2 \cos(\omega t), \\ m\ddot{y}_1 + c(\dot{y}_1 - \dot{y}_2) + k(y_1 - y_2) = F_{fy}(y_1, y_2) + mu\omega^2 \sin(\omega t) - mg, \\ c(\dot{x}_2 - \dot{x}_1) + k(x_2 - x_1) = P_x(x_2, y_2, \dot{x}_2, \dot{y}_2), \\ c(\dot{y}_2 - \dot{y}_1) + k(y_2 - y_1) = P_y(x_2, y_2, \dot{x}_2, \dot{y}_2). \end{cases}$$

As to the oil film forces, short bearing approximation is considered. Oil film pressure p is integrated in all surface of the bearing, and the Sommerfeld boundary condition is used. The components of oil film force in x and y direction can be obtained [8] as

$$P_x(x, y, \dot{x}, \dot{y}) = -\eta\pi R l^3 \times \left[\frac{wy + 2\dot{x}}{2(c_1^2 - x^2 - y^2)^{3/2}} + \frac{3x(x\dot{x} + y\dot{y})}{(c_1^2 - x^2 - y^2)^{5/2}} \right],$$

$$P_y(x, y, \dot{x}, \dot{y}) = -\eta\pi R l^3 \times \left[\frac{2\dot{y} - wx}{2(c_1^2 - x^2 - y^2)^{3/2}} + \frac{3y(x\dot{x} + y\dot{y})}{(c_1^2 - x^2 - y^2)^{5/2}} \right],$$

where η is the oil viscosity, R the bearing radius, and l the bearing length.

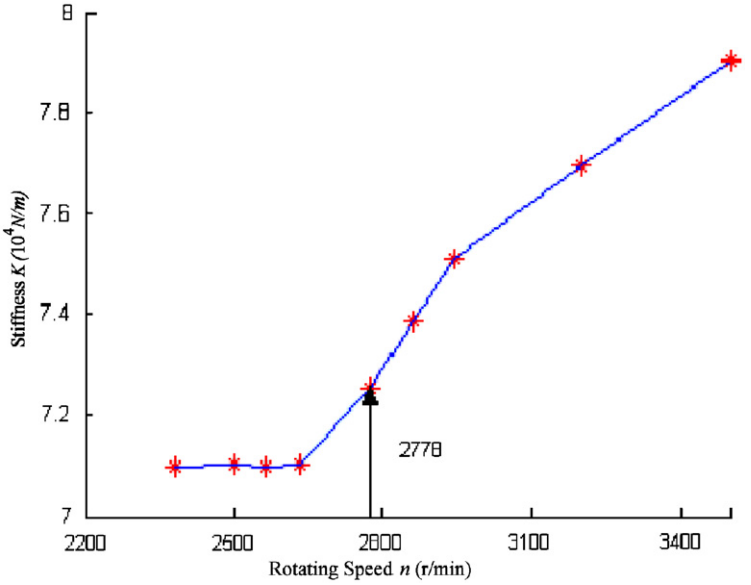

Fig. 3. Identification result of the transient stiffness.

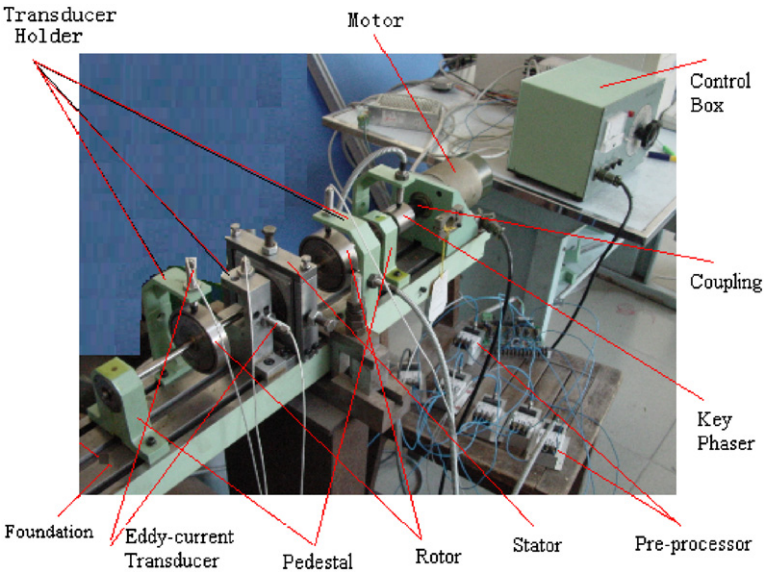

Fig. 4. Experiment arrangement of the rub–impact rotor system.

For this case, the vibration responses from $n = 2500$ rev/min to $n = 3500$ rev/min are calculated. The result shows that rub–impact begins to occur at a time about when $n = 2630$ rev/min. Fig. 3 shows the identification results of the transient stiffness, and a conclusion similar to that of Example 1 can be obtained. The transient stiffness basically does not change when there is no rub–impact, but keeps on increasing with the rub–impact aggravating, which again proves that the rotor has stiffening effect when rub–impact occurs.

4. Identification of transient stiffness based on experiment data

The experimental test rig is shown in Fig. 4. A coupling is connected between the motor and the shaft. The test rig, with simple structure, can be operated reliably in a wide speed range. The rated current of the electric

motor is 2.5 A, and the output power is 250 W. The rotating speed can be adjusted between 0~10,000 rev/min and the rate of the speed increase can reach to 800 rev/min. The rig can be installed with three rotors at the most. The eddy current transducers are used to measure the vibration displacements of the rotor and the number of measurement point is determined by the disk number. One measuring point in x and y directions, respectively, can be installed in every disk. There are different options for rigid coupling, half-flexibility coupling and flexibility coupling. Therefore, different testing requirement could be met.

Previous experimental investigations for the rub–impact rotor systems usually use the way of the point contact. In such manner, a rub screw holder is fixed at a certain position. Then the electric motor is started to operate at the experimental speed. The distance between the rub screw and the shaft is adjusted to an appropriate value until the rub impact is observed. Finally, the anti-looseness wing nut is tightened. However, this kind of simulation does not agree with the most cases of the real rotor-to-stator rub–impact and the experiment cannot simulate the condition of the full rub. Also the damage to the shaft will be caused in this kind of experiment and the experiment can only last for a short period of time. In order to better simulate the real process of the rub–impact, in our experiment we have designed a special structure of stator that can make it possible to perform a full rub experiment, as shown in Fig. 5. It is easy for the stator to be installed or detached. The clearance between the rotor and stator is adjustable to meet different experiment conditions.

In order to reduce the wear of the disks, the soft aluminium alloy is used to make the inner part of the stator. Three sizes of the inner stator were designed to simulate different clearances of 0.4, 0.6 and 0.8 mm, respectively. Four bolts were used to fix the inner stator and the stator holder tightly. The holder was a kind of the steel structure to increase the stiffness of the whole stator. Thus not only can the concentricity of the stator and the rotor (uniform clearance along the circumferential direction between the rotor and the stator) be adjusted, but also the size of the clearance can be adjusted by the change of different inner stators to control the time when the rub–impact occurs and the severity of the rubbing.

Based on the experimental vibration data, the above-mentioned method of transient stiffness is used to perform the parameter identification, so the transient stiffness can be obtained. By observing the change trend of the transient stiffness, whether the system has rub–impact or not can be judged. When rub–impact occurs, the relation between the transient stiffness and the severity of rub–impact can be investigated.

The experiment rig includes a single disk rotor supported in both ends by oil film bearings. System parameters are concentrated mass $m = 0.6143$ kg, shaft length $l = 0.340$ m, inner diameter of the stator is 76.72 mm, and outer diameter of the disk is 76.2 mm.

In the experiment, the rotating speed is increased from $n = 1857$ to $n = 2941$ rev/min. When the speed is at about $n = 2564$ rev/min, the rub–impact occurs between the disk and the stator. With the speed increasing, the

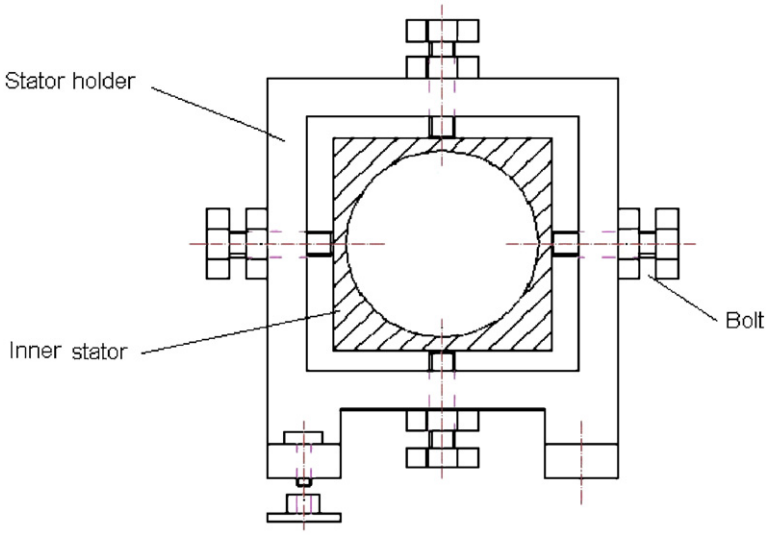

Fig. 5. Diagram of the stator structure.

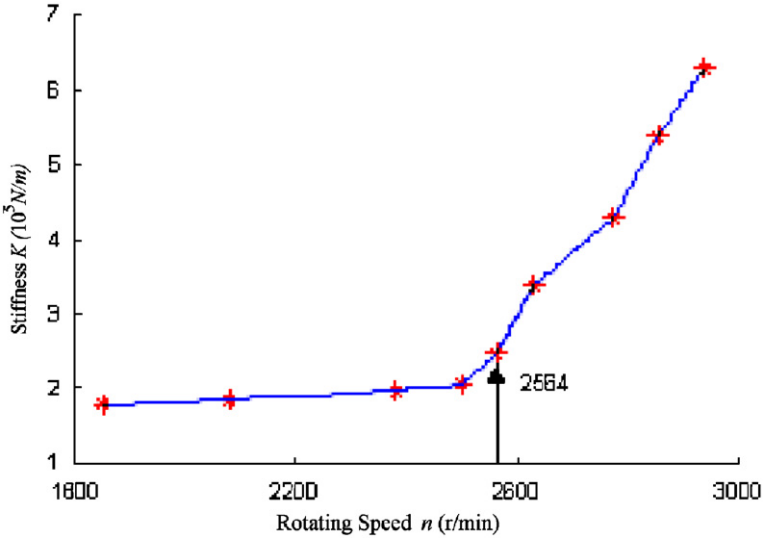

Fig. 6. Identification result of the transient stiffness.

rub–impact keeps aggravating. The identification result of the transient stiffness is shown in Fig. 6. It is obvious that the transient stiffness basically does not change when there is no rub–impact, but keeps on increasing with the rub–impact aggravating when the speed increasing. A similar trend can be obtained for the identification results of the damping coefficient.

5. Conclusions

A parameter called transient stiffness is introduced in this paper to describe quantitatively the rub–impact interaction in a rotor system. With the method of the model based parameter identification, the vibration signals are used to identify the change trend of the transient stiffness, thereby to judge whether the system has rub–impact or not. By the results of numerical simulation and experimental test, the following conclusions can be drawn:

Whether the rotor system is supported in both ends rigidly or by oil film bearings, the rotor system has certain degree of the stiffening effect after rub–impact occurs, and the value of the transient stiffness increases with the rub–impact aggravates.

The change trend of the transient stiffness can be used to judge the occurrence and the severity of the rub–impact in the system. Identification results by both numerical simulation and experimental test have verified that the method is simple and effective. However, the method can only be applied for the system where vibration signals are measurable.

Acknowledgements

This research is supported by Natural Science Foundation of China (Grant no. 50425516) and the 863 High-Tech Scheme (2006AA04Z438) by the Ministry of Science and Technology.

References

[1] F.F. Ehrich, High order subharmonic response of high speed rotors in bearing clearance, *Journal of Vibration, Acoustics, Stress and Reliability in Design—Transactions of the ASME* 110 (1988) 8–16.

[2] S. Zhang, Q. Lu, Q. Wang, Analysis of rub–impact events for a rotor eccentric from the case, *Journal of Vibration Engineering* 11 (4) (1998) 492–496.

[3] X. Liu, Q. Li, S. Yang, The stability and Hopf bifurcation in the annular impact rub of rotating machinery with imbalance, *Journal of Vibration Engineering* 12 (1) (1999) 40–46.
[4] X. Dai, X. Zhang, Z. Jin, Experiments of partial and full rotor/stop rubbing, *Journal of Aerospace Power* 15 (4) (2000) 405–409.
[5] X. Li, T. Shi, S. Yang, Nonlinear dynamics of rotor rubbing against rotor–stator on flexible supports, *Journal of Vibration Engineering* 14 (3) (2001) 303–308.
[6] W. Lu, Dynamic Characteristics and Fault Diagnosis of Rubbing Fault in Rotating Machinery, PhD dissertation, Tsinghua University, Beijing, 2002.
[7] F. Chu, X. Tang, Y. Tang, Stability of a rub–impact rotor system, *Journal of Tsinghua University (Science and Technology)* 40 (4) (2000) 119–123.
[8] F. Chu, Z. Zhang, Periodic, quasi-periodic and chaotic vibrations of a rub–impact rotor system supported on oil film bearings, *International Journal of Engineering Science* 35 (10–11) (1997) 963–973.